

# APPLICATIONS BULLETIN

## Mechanical Properties of Cementitious Materials

### //// Introduction

This Applications Bulletin focuses on some of the applications being developed by the Civil Engineering Dept at MIT (Massachusetts Institute of Technology), for whom CSM Instruments developed a novel humidity-controlled nanoindentation system. This group is centered around the study of geomaterials or natural composites, i.e., materials which occur naturally and have complex heterogeneous structures. Examples of such materials are cement pastes (used for concrete) and shales (which cover oilfields).

The mechanical properties of cement have been gradually improved over the last decades, but this has been achieved more by trial and error than by an in-depth understanding of what is happening at the micro- and nanoscales. The setting of cement is not, as sometimes believed, a drying process; in fact, it is the exact opposite. When cement is mixed with water, it undergoes a dissolution reaction generating calcium, silicate and aluminate ions in the interstitial solution. New products (hydrates) then precipitate when their solubility limit is reached and after a nucleation period. In a common cement, such as Portland cement, this dissolution-diffusion-precipitation process produces calcium silicate hydrate (C-S-H) and calcium hydroxide (Portlandite). During hydration the slurry coagulates once the cement is mixed with water, after which setting occurs and some proportion of the anhydrous cement is transformed into C-S-H and other hydrates.

C-S-H is a nonstoichiometric compound and the average Ca/Si ratio in ordinary hardened cement paste is around 1.7. It has a layered crystal structure akin to that of the mineral tobermorite, which is why this mineral is often used as a model material as it is analogous to the main hydrated phase of cement paste and can be artificially produced. The multiscale heterogeneity of concrete ultimately determines its *in vivo* mechanical performance (stiffness, strength) and degradation (damage, fracture, failure). The microstructure can be divided into four levels as shown in Fig. 1, from the scale of mortar ( $10^{-2}$  m) down to the C-S-H solid phase ( $10^{-10}$  m) which represents the smallest material length scale that is currently accessible by mechanical testing (nanoindentation). By experimentally investigating the mechanical properties of cement paste at different length scales provides a means of correlating such microscale properties to macroscale applications.

The requirement for in-situ analysis of chemically complex phases obviates conventional mechanical testing of large specimens representative of these material components. Thus nanoindentation can be used as a 2D mapping tool for examining the properties of constituent phases independently of each other.

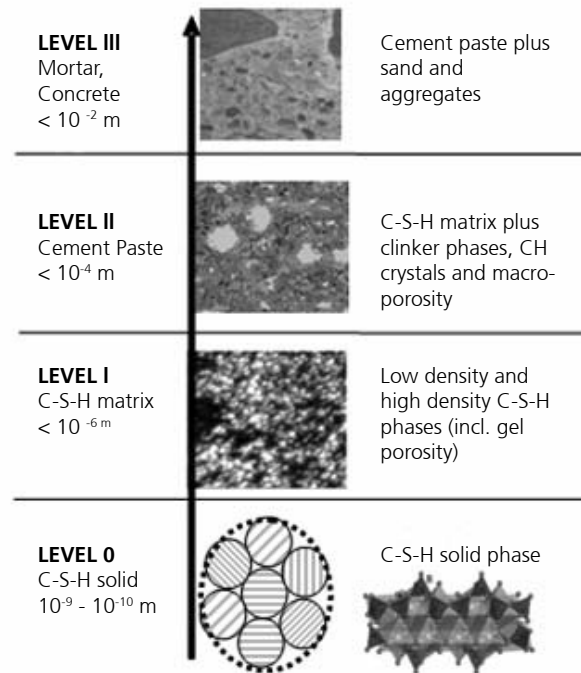
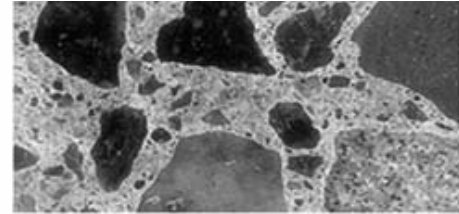


Fig. 1: Four-level microstructure of cement-based composite materials

### //// Grid Indentation Technique

A novel grid-indentation technique can not only be used to obtain key mechanical properties of heterogeneous materials (such as C-S-H) at a particular length scale, but can also provide access to the volume fractions of independent phases. Consider a material to be composed of two phases of different mechanical properties and characterized by a length scale  $D$ , as described in Fig. 2. If the indentation depth is much smaller than the characteristic size of the phases,  $h < D$ , then a single indentation test gives access to the material properties of either phase 1 or phase 2. If, in addition, a large number of tests is carried out on a grid (or matrix) defined by a grid spacing  $L$  that is larger than the characteristic size of the indentation impression, so as to avoid interference in between individual indentation tests, and much larger than the characteristic size of the two phases, then the probability of encountering one or the other phase is

equal to the surface fraction occupied by the two phases on the indentation surface. On the other hand, an indentation test performed to a maximum indentation depth that is much larger than the characteristic size of the individual phases,  $h > D$ , senses the average response of the composite material, and the properties extracted from such an indentation experiment are representative in a statistical sense of the average properties of the composite material.

Such large matrices of indentations provide a statistical analysis comprising distributions and their derivatives (e.g., histograms or frequency diagrams) of mechanical properties determined by a large number of indentation experiments at a specific scale of material observation defined by the indentation depth. Hardened concrete always contains a significant fraction of liquid water from the capillary condensation of water vapor in the intergranular pores, so it is of particular interest to perform grid-indentations with accurate Relative Humidity (RH) control in order to quantify the influence of water fraction on mechanical properties. Such was the motivation for designing a fully-automated nanoindentation instrument, capable of making hundreds to thousands of indentations whilst maintaining the ambient humidity to an accuracy of  $\pm 0.1$  % RH.

### //// Experimental Setup

The basic configuration of the humidity control system is shown in Fig. 3. The Nano Hardness Tester (NHT), video optical microscope and XYZ sample displacement stage are housed within the inner chamber which is controlled by a closed loop air conditioning system and can be sealed at any moment with valves V1 and V2. These valves are opened to allow the inner chamber to acclimatize to a predefined humidity level, after which they are closed to seal the chamber during the nanoindentation load-depth cycle and prevent any movement of air which could perturb the ultra-sensitive experiment. The downside of switching-off the flow of controlled air is that the humidity level will tend to drift during the test cycle, owing to losses through the chamber walls.

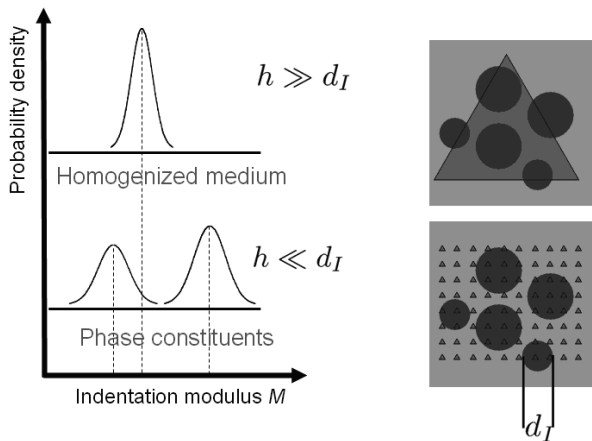


Fig. 2 : Schematic of the principle of the grid indentation technique for heterogeneous materials. Small indentation depths allow the determination of phase properties, while larger indentation depths lead to the response of the homogenized medium.

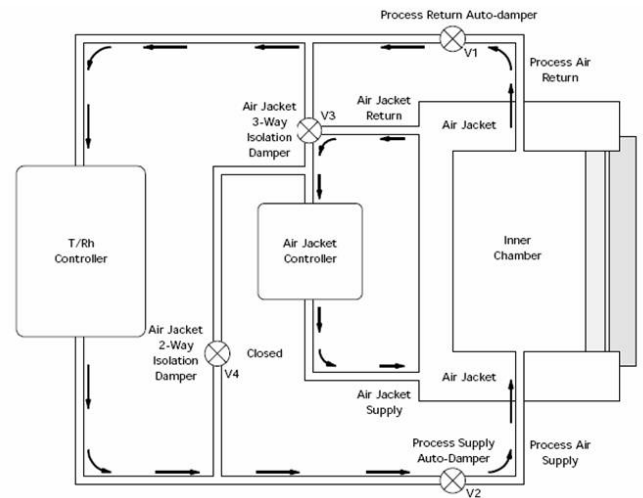


Fig. 3: Schematic of the humidity system with independently controlled inner chamber and outer air jacket. The system operates over the ranges 10 – 40 °C and 30 – 90 % RH.

To prevent such losses, the inner chamber is surrounded by an outer air jacket which is independently temperature-controlled, via valves V3 and V4. By maintaining a layer of air whose temperature is stable means that a predefined RH value can be kept constant for adequate time periods (several minutes), sufficient for performing an indentation test.

When running a large matrix of indentations, the control valves V1 and V2 are operated between each indentation cycle, allowing hundreds of indentations to be made under perfectly controlled environmental conditions. The system operates over the ranges 10 – 40 °C and 30 – 90 % RH as summarized in Fig. 4. The actual dewpoint in the inner chamber is accurately monitored at all times to prevent condensation which might damage the most sensitive parts of the nanoindentation and XYZ positioning system. In addition, condensation must be prevented as this would prevent high-quality imaging through the integrated optical microscope.

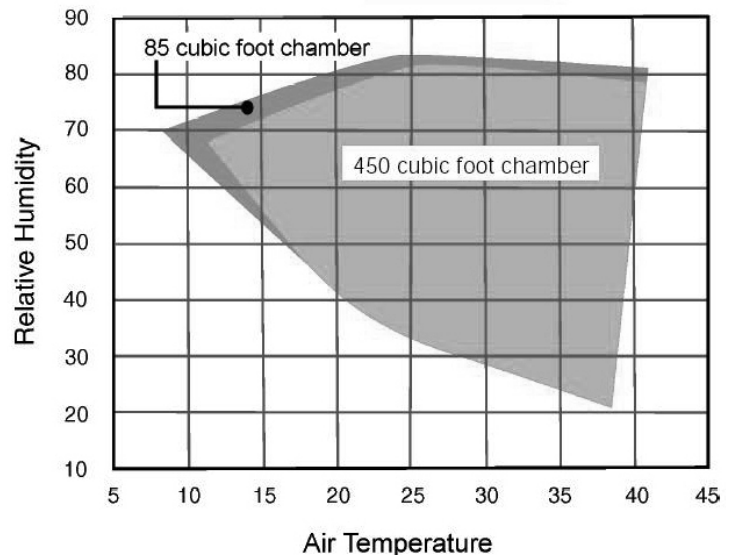


Fig. 4: Operating range for the system shown in Fig. 3, showing the relationship between the temperature and humidity.

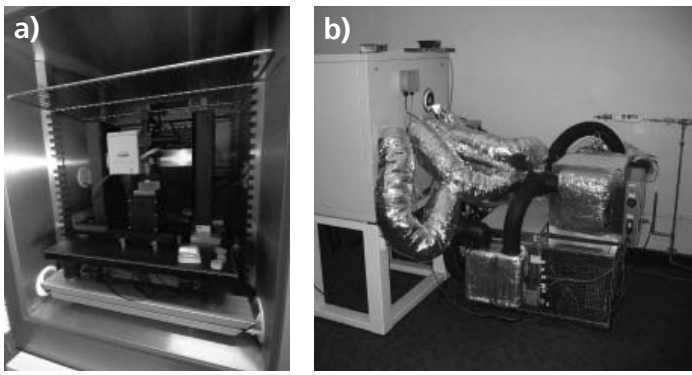


Fig. 5: Inner chamber (a) showing the nanoindentation head (left) and the integrated optical video microscope (right) mounted over the automated XYZ sample displacement stage. The humidity and temperature controller is shown in (b).

The actual layout of the system is shown in Fig. 5 and the main door is equipped with a sealed window for inspection and a glovebox for manipulating samples whilst maintaining controlled conditions. The XYZ sample displacement stage and the optical video microscope are both separately enshrouded by water-resistant plastic housings to prevent any effect of condensation at elevated humidity levels.

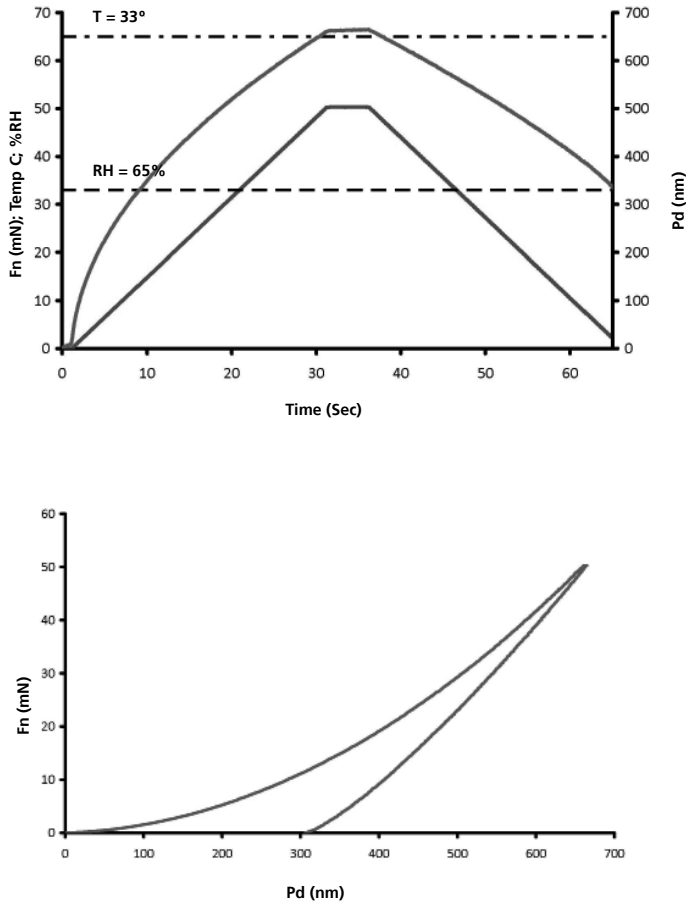


Fig. 6: Typical nanoindentation measurement file showing temperature and humidity signals superimposed over the load-unload cycle. This example shows an indentation on fused silica at 33°C and 65% RH with maximum load 50 mN

A typical nanoindentation measurement is shown in Fig. 6 with corresponding temperature (T) and humidity signals recorded over the measurement period (65 seconds) confirming that both T and RH are perfectly maintained during the test cycle.

Sample preparation can be an issue with cementitious materials which are composed of very different constituent phases. Obviously, for measuring the surface mechanical properties of individual phases, the indentation penetration depth must remain significantly smaller than the phase size. In reality, with depths typically < 200 nm, the surface roughness of the polished section must be very low otherwise there will be significant standard deviation in the results.

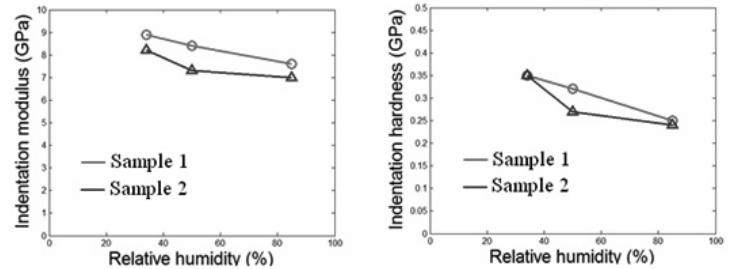


Fig. 7: Indentation hardness and modulus plotted as a function of relative humidity (35 – 90%) for 2 tobermorite samples

Many concrete mixtures also contain air voids from air which gets trapped during mixing. These microscopic voids provide free space to relieve hydraulic pressure when concrete freezes, otherwise it may crack. It may be important to maintain the true void structure throughout the preparation process. Some investigators may actually impregnate the surface with a low viscosity epoxy so that the epoxy will readily penetrate the voids and cracks, thus preventing collapse of the void walls during polishing.

The actual polishing method will be determined by the constituent phases present and their relative wear rates which will determine which abrasive particle size is most suited. If the abrasive paper, speed of polishing and liquid medium are not controlled adequately, then preferential polishing of softer phases will often occur, causing excessive roughness which will cause error in the mechanical properties measured.

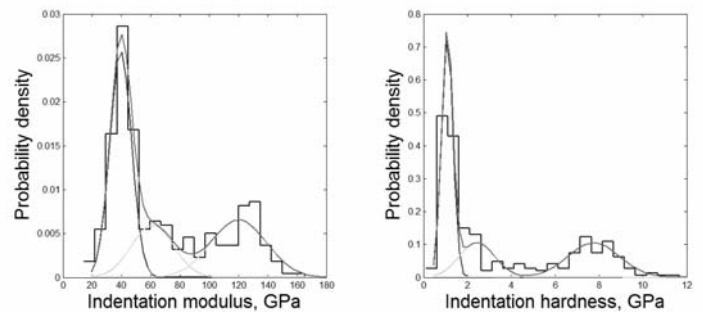


Fig. 8: Indentation hardness and modulus density groups for a tobermorite sample, summarized from a matrix of 300 nanoindentations (max load 5 mN). Note the presence of 3 phases.

Some typical nanoindentation results on a tobermorite sample are shown in Figures 7 and 8, the former showing hardness and modulus as a function of relative humidity, the latter showing the Probability Density plots (histograms) of hardness and modulus. Note that from a nanoindentation matrix comprising 300 equispaced indents, three distinct phases are clearly distinguishable (a 3-Gaussian fit).

Hydrated cement pastes can be confidentially divided into at least 3 significant mechanical phases: two hydrated phases and the remaining unhydrated clinker. The two hydrated phases are a low density C-S-H phase and a high density C-S-H phase. In Fig. 8, the first peak has a Hardness (H) of 1.2 GPa and Modulus (E) of 41 GPa, the second peak has H = 2.3 GPa and E = 62 GPa and the third peak has H = 7.8 GPa and E = 120 GPa.

### //// Conclusions

The grid indentation technique combined with the ability to measure properties at the nanoscale in a controlled humidity environment has been shown to provide a wealth of information in cementitious materials:

- The mechanical properties (H, E, packing density, volume fraction, etc.).
- Homogenized indentation modulus (calculated by combining the surface volume fractions of each phase with their respective moduli).
- The porosity distribution within a sample.

Further optimization of the technique will allow in situ mechanical properties to be extracted at the micro- and nanoscales, providing a valid method of correlating individual phase properties with bulk response. For a more in-depth explanation of the grid indentation technique and some examples on other types of materials (including metal composites), see Ref. 7.

### //// Acknowledgements

Prof. Franz-Josef Ulm (MIT Civil Eng.), Matthieu Vandamme (Ecole des Ponts, Paris) and Chris Bobko (North Carolina State Uni.) are acknowledged for sharing their interesting results.

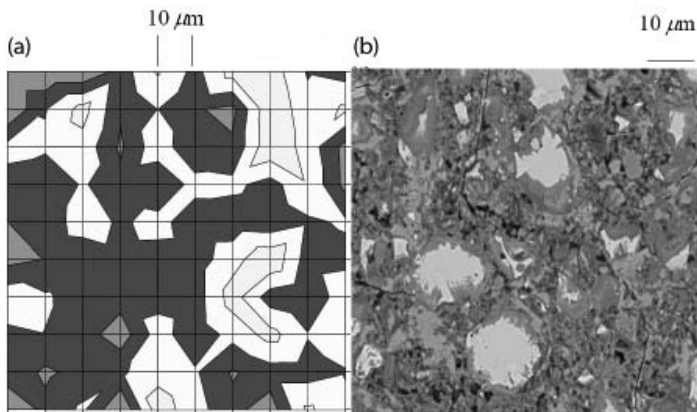


Fig. 9: Elastic modulus map (a) on a C-S-H sample for a 100 indent nanoindentation matrix with spacing between indents of 10 µm. A similar magnification Scanning Electron Microscope (SEM) image is shown in (b) for comparison.

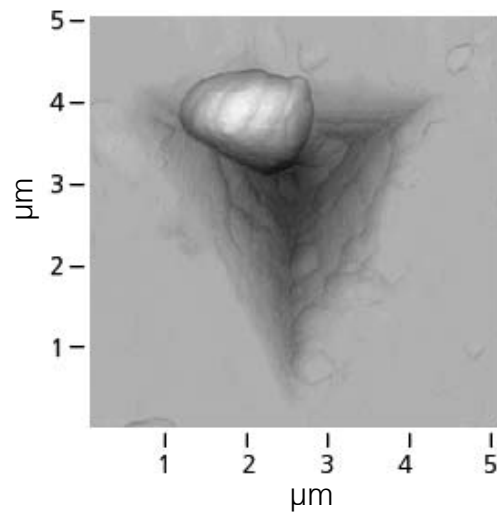


Fig. 10: Scanning Force Microscope (SFM) image of a nanoindentation in a C-S-H phase made to a depth of 500 nm using a Berkovich diamond indenter.

### //// References

1. R. J. -M Pellenq and H Van Damme, MRS Bulletin, (May 2004) 319 – 323
2. G. Constantinides, F. J. Ulm and K. J. Van Vliet, Materials and Structures, 36 (2003) 191 - 196
3. F. J. Ulm, G. Constantinides and F. H. Heukamp, Concrete Science and Engineering, 37 (2004) 43 – 58
4. G. Constantinides and F. J. Ulm, Cement and Concrete Research, 34 (2004) 67 – 80
5. G. Constantinides, K. S. Ravi Chandran, F. J. Ulm and K. J. Van Vliet, Materials Science and Engineering, A 430 (2006) 189 - 202
6. G. Constantinides and F. J. Ulm, Journal of Mechanics and Physics of Solids, 55 (2007) 64 – 90
7. N. X. Randall, M. Vandamme and F. J. Ulm, J. Mater. Res., Vol. 24, No. 3 (March 2009) 679 - 690
8. M. Miller, C. Bobko, M. Vandamme and F.-J. Ulm, Cement and Concrete Research 38 (4) (2008) 467-476



This Applications Bulletin is published quarterly and features interesting studies, new developments and other applications for our full range of mechanical surface testing instruments.

Editor Dr Nicholas X. RANDALL

Should you require further information, please contact:

CSM Instruments  
Rue de la Gare 4  
CH-2034 Peseux  
Switzerland

Tel: + 41 32 557 5600  
Fax: +41 32 557 5610  
info@csm-instruments.com  
www.csm-instruments.com